Chemistry–A European Journal

Research Article
doi.org/10.1002/chem.202404361

Chemistry Europe
European Chemical Societies Publishing

www.chemeurj.org

Synthesis and Redox Chemistry of Co_3E_4 (E = P, As) Clusters

Martin Piesch,[a] Sabrina B. Dinauer,[a] Christoph Riesinger,[a] Gábor Balázs,[a] and Manfred Scheer*[a]

Dedicated to Professor Rainer Winter on the occasion of his 60th birthday

The synthesis of the cluster complexes $[(Cp'''Co)_3(\mu_3,\eta^2{:}\eta^2{:}\eta^2\text{-}E_3)(\mu_3\text{-}E)]$ (E = P (**3**), As (**4**)) starting from the anionic triple-decker complexes $[K(18cr6)(dme)_2][(Cp'''Co)_2(\mu,\eta^4{:}\eta^4\text{-}E_4)]$ (E = P (**1**), As (**2**)) by electrophilic quenching with the Co dimer $[(Cp'''CoCl)_2]$ is reported. Both complexes show a distinct redox chemistry, which was first investigated by cyclic voltammetry. Subsequently, the monoanions $[K(L)(sol)_n][(Cp'''Co)_3(\mu_3,\eta^2{:}\eta^2{:}\eta^2\text{-}E_3)(\mu_3\text{-}E)]$ (E = P, L = 18cr6, sol = dme, n = 2 (**5**), E = As, L = 2,2,2-crypt, n = 0 (**6**)), the monocations $[(Cp'''Co)_3(\mu_3,\eta^2{:}\eta^2{:}\eta^2\text{-}E_3)(\mu_3\text{-}E)][Al]$ (E = P (**7**), As (**8**)) and the dications $[(Cp'''Co)_3(\mu_3,\eta^3{:}\eta^3{:}\eta^3\text{-}E_4)][TEF]_2$ (E = P (**9**), As (**10**)) could be realized experimentally and isolated in moderate to good yields. All compounds were characterized by single crystal X-ray structure analysis, NMR and EPR spectroscopy, mass spectrometry and elemental analysis.

Introduction

Due to their complex redox behaviors and confined coordination sphere, multi-metallic systems have attracted great attention not only for catalytic systems.[1] Despite their utilization in numerous fields, a controllable synthesis of many transition metal clusters remains a challenge and most of them are solely investigated by density functional theory calculations.[2] For the synthesis of $[(Cp^RCo)_nE_m]$ (E = P, As) cluster or cage complexes, only a few different routes are described in the literature. *Scherer et al.* reported the thermolysis and photolysis of $[Cp^RCo(CO)_2]$ ($Cp^R = C_5Me_5$, C_5Me_4Et, $C_5{}^tBu_3H_2$) with white phosphorus and yellow arsenic, respectively.[3] By this approach, transition metal clusters such as $[(Cp^RCo)_2(E_2)_2]$ (E = P, As), $[(Cp'''Co)_3P_8]$, $[(Cp'''Co)_3P_2]$ (**I**, Figure 1), $[(Cp^RCo)_2As_6]$, and $[(Cp^RCo)_3As_6]$ are obtained more or less selectively. Alternatively, pentaphosphaferrocene $[Cp^*Fe(\eta^5\text{-}P_5)]$ can be used as a phosphorus source. Its thermolysis with $[Cp^RCo(CO)_2]$ and $[\{Cp^RFe(CO)_2\}_2]$, respectively, leads to the Co cluster $[(Cp^RCo)_4P_4]$ (**II**) and $[(Cp^RCo)_3P_2]$ (some representatives are shown in Figure 1) in addition to the mixed metal clusters $[(Cp^*Fe)_2(Cp^RCoP_4)]$, $[(Cp^*Fe)(Cp^RCo)_2(P_4)(P)]$ and $[(Cp^*Fe)(P_5)(Cp^RCo(CO))\{Cp^RCo)_2(CO)\}]$.[4] *Fenske et al.* developed another approach for polynuclear cobalt complexes by reacting the functionalized Zintl phase $[E_7(SiMe_3)_3]$ (E = P, As) with *in situ* generated $[(Cp^*CoCl)_2]$ to obtain $[(Cp^*Co)_3(P_4)(P_2)]$ (**III**) and $[(Cp^*Co)_3As_6]^{2+}$ (**IV**), respectively (Figure 1).[5] However, the subsequent reactivity of these homometallic transition metal complexes was not investigated except for the redox chemistry of the isostructural prismane cluster $[\{Cp^*Fe\}_3(\mu_3,\eta^{4:4:4}\text{-}As_6)]$ to elucidate the structural features of the respective products.[6]

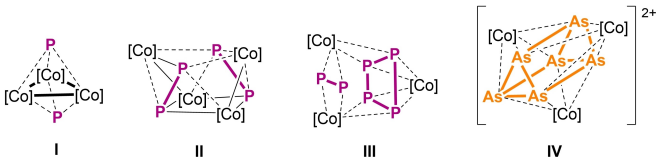

Figure 1. Selected examples of $[(Cp^RCo)_nE_m]$ complexes.

In contrast to the rather harsh reaction conditions of the photolysis and thermolysis reactions mentioned before, $[(Cp'''Co)_2(\mu,\eta^4{:}\eta^4\text{-}C_7H_8)]$ was used to perform reactions with white phosphorus and yellow arsenic, respectively, under mild conditions even at very low temperatures. Depending on the reaction conditions, either products similar to **I** and **II** were obtained, or even larger E_n-rich complexes of cobalt with up to 24 P and 12 As atoms, respectively.[7] Recently, the synthesis of the mixed metal triple-decker complex $[[Cp^*Fe)(Cp'''Co)(\mu,\eta^5{:}\eta^4\text{-}P_5)]$ was reported, which was obtained by the reaction of $[Cp^*Fe(\eta^5\text{-}P_5)]$ with $[(Cp'''Co)_2(\mu,\eta^4{:}\eta^4\text{-}C_7H_8)]$ or alternatively by electrophilic quenching of the reduced pentaphosphaferrocene derivative $[(Cp^*Fe)_2P_{10})]^{2-}$ with $[(Cp'''CoCl)_2]$.[8] Using transition metal halide dimers of the type $[(Cp'''MX)_2]$ (M = Cr, Mn, Fe, Ni; X = Br, Cl, I) in the reaction with *in situ* generated $[Cp^*Fe(\eta^5\text{-}P_5)]^{2-}$ is another approach to access triple-decker complexes and homo and hetero metallic cage compounds of the type $[(Cp^*Fe)(Cp'''M)_nE_5]$ (n = 1, 2).[9] Herein, we report about a synthetic principle of using the reduced cobalt triple-decker $([K(18cr6)(dme)_2][(Cp'''Co)_2(\mu,\eta^4{:}\eta^4\text{-}E_4)]$ (E = P (**1**), As (**2**))[10] for the generation of novel homometallic Co polypnictogen cluster complexes. Moreover, the enhanced reactivity of the obtained $\{Co_3E_4\}$ clusters $[(Cp'''Co)_3(\mu_3,\eta^2{:}\eta^2{:}\eta^2\text{–}E_3)(\mu_3\text{–}E)]$ (E = P, As) regarding their versatile redox chemistry is reported.

[a] M. Piesch, S. B. Dinauer, C. Riesinger, G. Balázs, M. Scheer
Institute of Inorganic Chemistry, University of Regensburg, 93040 Regensburg, Germany
E-mail: manfred.scheer@chemie.uni-regensburg.de

Supporting information for this article is available on the WWW under https://doi.org/10.1002/chem.202404361

Results and Discussion

The starting complexes $[(Cp'''Co)_2(\mu,\eta^2{:}\eta^2{-}E_2)_2]$ (E = P (**A**), As (**B**)), which are available in gram scale, can easily be reduced to the extremely air- and moisture-sensitive anionic complexes $[K(18c6)(dme)_2][(Cp'''Co)_2(\mu,\eta^4{:}\eta^4{-}E_4)]$ (E = P (**1**), As (**2**)), which serve as starting materials for further cluster formations.[10] Alternatively, complexes **1** and **2** can be generated *in situ* by the reduction of **A** or **B** with KC_8 without the use of 18c6. These compounds can then be quenched electrophilically with $[\{Cp'''Co(\mu\text{-}Cl)\}_2]$ at room temperature under release of potassium chloride to obtain the cluster complexes $[(Cp'''Co)_3(\mu_3,\eta^2{:}\eta^2{:}\eta^2{-}E_3)(\mu_3{-}E)]$ (E = P (**3**), As (**4**)) in crystalline yields of 49% (**3**) and 51% (**4**), respectively, after column chromatographic workup (Scheme 1).According to the Wade Mingos[11] rules complexes **3** and **4** account both for 9 skeletal electron pairs (18 skeletal e^-), and thus can be formulated as *nido* clusters. A description using the sum of valence electrons provides 62 valence electrons for clusters **3** and **4**, respectively.

Crystals of **3** and **4** suitable for single crystal X-ray structure analysis were obtained from concentrated solutions in CH_2Cl_2 layered with CH_3CN at −30 °C. The molecular structures in the solid state are depicted in Figure 2.

Both compounds crystallize in the orthorhombic space group *Pbca* with almost identical cell parameters. The structures in the solid state reveal a trinuclear cluster consisting of three {Cp'''Co} fragments connected by an E_3 ligand in an $\eta^2{:}\eta^2{:}\eta^2$ mode and an E_1 ligand in a μ_3 binding mode. The central Co_3E_4 core is mostly built up by triangular faces of the Co_3E_3 unit capped by the E_1 ligand. A strong metal-metal interaction between Co1 and Co2 (2.7258(4) Å in **3**, 2.8193(6) Å in **4**) is present, which is also indicated by the Wiberg Bond Indices (WBIs) (0.49 (**3**) and 0.33 (**4**)) and the electron density between them as shown by the occupied frontier orbitals (BP86/def2-SVP level of theory, cf. Figure S40 and S41)). The bond distances within the *cyclo*-E_3 ligands are in the range of elongated single bonds (P–P bonds 2.2960(5)–2.3787(5) Å in **3**, As–As bonds 2.5407(6)–2.5974(5) Å in **4**), which is also consistent with the WBIs (P– bonds: 0.53–0.63, As–As bonds: 0.58–0.61).[12] The single E_1 ligand is located asymmetrically over the *cyclo*-E_3 ligand with two shorter E–E distances (P1–P3 2.6341(5) Å, P1–P4 2.6564(7) Å, As1–As3 2.8688(7) Å, As1–As4 2.8511(7) Å) and one longer distance (P1–P2 3.1647(5) Å, As1–As2 3.4065(6) Å). The WBIs for these pairs reveal an interaction between P1–P3 (0.25), P1–P4 (0.28), As1–As3 (0.36) and As1–As4 (0.33), but no interaction for P1–P2 (0.05) and As1–As2 (0.09). The ^1H NMR spectra of **3** and **4** in solution each reveal three singlets at δ = 4.86, 1.52 and 1.33 ppm (**3**) and δ = 4.56, 1.54 and 1.38 ppm (**4**) with an integral ratio of 6:54:27 corresponding to three equivalent Cp''' ligands. In the $^{31}P\{^1H\}$ NMR spectrum of **3**, two singlets with an integral ratio of 1:3 at δ = 648.0 and 358.5 ppm are detected. Upon cooling both singlets broaden and the signal at δ = 358.5 ppm splits at 193 K into two very broad singlets in an integration ratio of roughly 1:2 (see Figure S11). This shows that the P atoms of the *cyclo*-P_3 unit get inequivalent at that temperature. Unfortunately, due to the broadness of the signals and poor signal to noise ratio, this splitting cannot unambiguously be attributed to a restricted rotation of the Cp''' ligand or to the lowering of the symmetry of the *cyclo*-P_3 ligand. Additionally, the redox properties of **3** and **4** were investigated by cyclic voltammetry in solution (Figure 3).

For **3**, one reversible oxidation process at −393 mV and one reversible reduction process at −1694 mV against $[Cp_2Fe]/[Cp_2Fe]^+$ are detected (see SI). In the voltammogram trace impurities of an unidentified species (marked with *) are present corresponding to the reversible processes at −1447, −656 and −187 mV. For **4**, two reversible oxidation processes at −569 and 69 mV and one electrochemically reversible reduction process at −1790 mV against $[Cp_2Fe]/[Cp_2Fe]^+$ are observed. Due to the very negative reduction potentials of **3** and **4**, potassium graphite was chosen as a suitable reducing agent for the experimental reduction. Reacting **3** and **4** with potassium graphite in the presence of 18c6 or 2,2,2-cryptand,

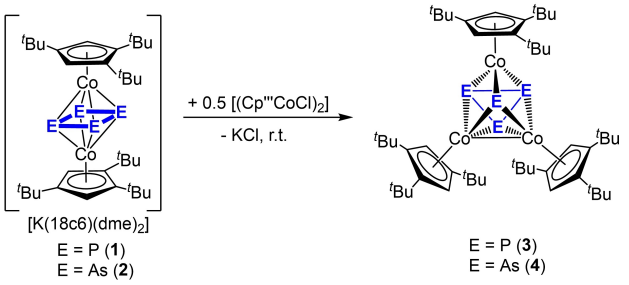

Scheme 1. Synthesis of the cage compounds **3** and **4**.

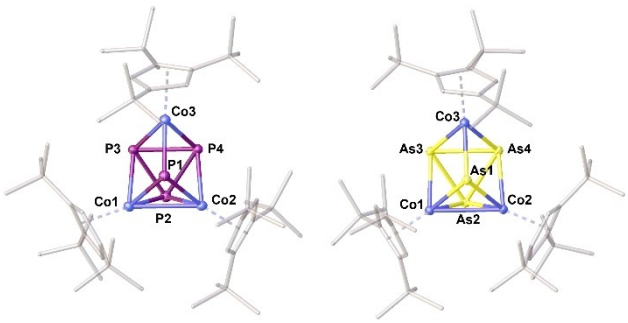

Figure 2. Molecular structures of **3** (left) and **4** (right) in the solid state. ADPs (anisotropic displacement parameters) are drawn at the 50% probability level. Hydrogen atoms are omitted for clarity.

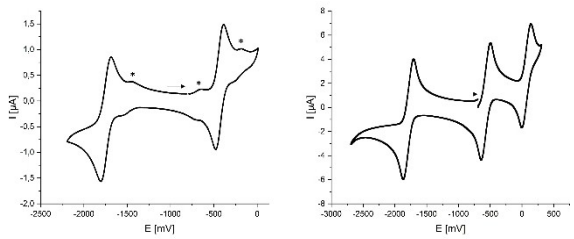

Figure 3. Cyclic voltammogram of **3** (left) and **4** (right) in thf versus $[Cp_2Fe]/[Cp_2Fe]^+$ (electrolyte $[^nBu_4N][PF_6]$, rate of feed: 100 mV/s. temperature: r.t.; processes marked with * correspond to trace impurities of an unidentified species).

respectively, results in the anionic complexes [K-(L)(sol)$_n$][(Cp'''Co)$_3$(μ_3,η^2:η^2:η^2-E$_3$)(μ_3-E)] (E = P, L = 18cr6, sol = dme, n = 2 (**5**), E = As, L = 2,2,2-crypt, n = 0 (**6**)) in crystalline yields of 49 % (**5**) and 61 % (**6**), respectively (Scheme 2).

Crystals suitable for single crystal X-ray structure analysis were obtained from concentrated solutions in dme (**5**) or thf (**6**) layered with *n*-hexane at −30 °C after a few days. The molecular structures of the anions of **5** and **6** in the solid state are depicted in Figure 4.

Both **5** and **6** respond to the reduction with solely a subtle change in the geometry. The Co1–Co2 distances in **5** and **6** are 2.9904(10) Å (**5**, WBI 0.27) and 3.1457(6) Å (**6**, WBI 0.23). Hence, the Co1–Co2 distance is elongated compared to **3** and **4**, displaying weak interactions in **5** and **6**. A weakening or cleavage of an M–M bond within a transition metal cluster was also reported upon reduction of [{Cp*Fe}$_3$(μ_3,$\eta^{4:4:4}$-As$_6$)].[6] All other Co–Co and E–E distances in **5** and **6** differ only slightly from the corresponding distances in **3** and **4**, respectively. The elongation of the Co1–Co2 distance agrees with the population of the LUMO of **3** and **4**, which both display a partially antibonding interaction between Co1 and Co2 (cf. Figure S40 and S41). Also, the HOMO orbitals of **5** and **6** are antibonding in relation to the electron density between the Co atoms (cf. Figure S42 and S43). In agreement with the addition of one electron, compounds **5** and **6** are evidenced as being paramagnetic by the broad and strongly shifted signals in the ^{1}H NMR spectra in solution and isotropic resonances in the EPR spectra (77 K, solid: **5**: g_{iso} = 2.081, **6**: g_{iso} = 2.121, cf. SI) with *g* values near to 2, indicative of one unpaired electron each. The effective magnetic moments in solution were determined by the Evans NMR method to be 2.04 μ_B (**5**) and 2.03 μ_B (**6**) each of which correspond to roughly one unpaired electron.

According to the low redox potentials for the oxidation processes of **3** and **4**, the Ag$^+$ salt of the weakly coordinating anion [FAl]$^-$ (= [FAl{OC$_6$F$_{10}$(C$_6$F$_5$)}$_3$]$^-$) was chosen as a suitable oxidizing agent. The oxidation of **3** and **4** with one equivalent of Ag[FAl] leads to the [FAl]$^-$ salts of the monocations [(Cp'''Co)$_3$(μ_3,η^2:η^2:η^2-E$_3$)(μ_3-E)][FAl] (E = P (**7**), As (**8**)) in crystalline yields of 48 % (**7**) and 52 % (**8**) (Scheme 3), under release of elemental Ag.

Crystals suitable for single crystal X-ray structure analysis are obtained after a few days from concentrated solutions in CH_2Cl_2 layered with toluene at −30 °C. The molecular structures in the solid state are depicted in Figure 5.

The degree of structural changes due to the oxidation is different for the phosphorus and arsenic compounds. For **7**, the structure in the solid state reveals only very small geometrical changes related to **3** (cf. SI). In the case of **8**, the geometry is significantly distorted. The Co1–Co2 distance is slightly elongated by 0.0441(6) Å in comparison to the starting complex **4**, while the Co1–Co3 distance is elongated by 0.1241(5) Å. The As1 atom is shifted more into the direction of As3 (decrease of As1–As3 distance by 0.215(5) Å, increase of the As1–As4 distance by 0.415(4) Å), resulting in an As1–As3 distance which is in the range of an elongated single bond (2.653(3) Å). This distance is comparable with the elongated As–As single bond in [(Cp*Co)(Cp*Co(CO))(μ,η^4:η^2-As$_4$)].[13] The As2–As3 and As3–As4 bonds are slightly elongated, while the As2–As4 bond remains unchanged. The corresponding DFT calculations do not completely agree with the observed structure in the solid state.

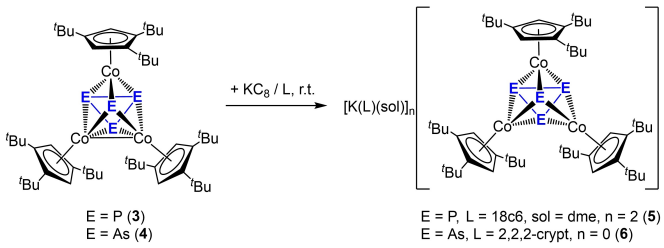

Scheme 2. Synthesis of the reduced complexes **5** and **6**.

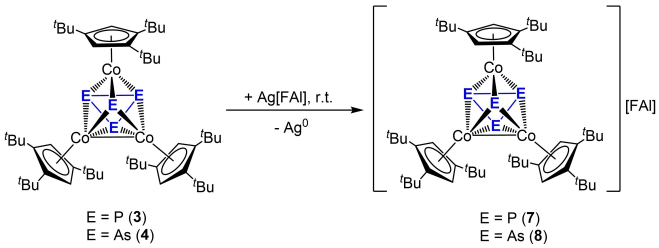

Scheme 3. Synthesis of the oxidized complexes **7** and **8**.

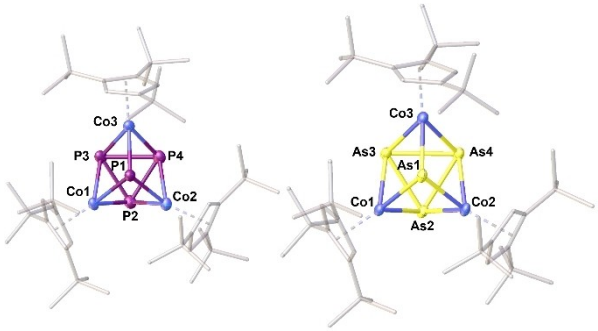

Figure 4. Molecular structures of the anions in **5** (left) and **6** (right) in the solid state. ADPs (anisotropic displacement parameters) are drawn at the 50 % probability level. Hydrogen atoms, cations and solvent molecules are omitted for clarity.

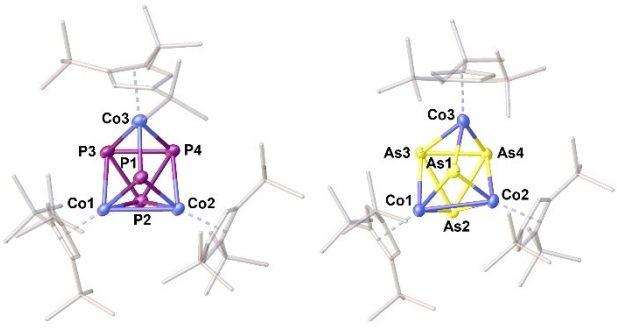

Figure 5. Molecular structure of the cations in **7** (left) and **8** (right) in the solid state. ADPs (anisotropic displacement parameters) are drawn at the 50 % probability level. Hydrogen atoms, anions and solvent molecules are omitted for clarity.

They support a similar, but less pronounced structural change, so that the larger distortion found experimentally might be attributable to packing effects in the experimental solid-state structure of **8** (cf. Figure S45). For compound **7**, the corresponding DFT calculations reveal an opposite change in the geometry (related to **3**), indicating a slight elongation of all Co–Co distances, which is not present in the experimental molecular structure of **7** (cf. Table S3). In agreement with the abstraction of one electron, compounds **7** and **8** are evidenced as being paramagnetic by broad and strongly shifted signals within the ^{1}H NMR spectra and the resonances found in the EPR spectra. While the X-band EPR spectra of **7** show an isotropic signal at room temperature (g_{iso} = 2.003) only in solution, the spectra of **8** show an isotropic signal at room temperature both in the solid state and in solution (g_{iso} = 2.142 and 2.003) splitting into a rhombic signal at 77 K in the solid state upon cooling (g_x = 2.2253, g_y = 2.1555, g_z = 2.0140, g_{iso} = 2.1316). The effective magnetic moments in solution were determined by the Evans NMR method to be 1.40 μ_B (**7**) and 1.47 μ_B (**8**), each of which correspond to roughly one unpaired electron. Additionally, in the ^{31}P{^{1}H} NMR spectrum of **7**, two very broad signals with an integral ratio of 1 : 3 at δ = 359.2 and 139.6 ppm are detected.

A further oxidation of **7** and **8** using another equivalent of Ag[FAl] in dichloromethane could not be achieved experimentally. In the reaction of **3** with two equivalents of Ag[FAl], solely the monocation of **5** could be identified. However, reacting **3** or **4** with two equivalents of Ag[TEF] (([TEF] = [Al{OC(CF$_3$)$_3$}$_4$]) in *ortho*-difluorobenzene provides access to the salts of the dications [(Cp‴Co)$_3$(μ_3,η^2:η^2:η^2-E$_3$)(μ_3-E)][TEF]$_2$ (E = P (**9**), As (**10**)) in crystalline yields of 63 % (**9**) and 80 % (**10**) (Scheme 4).

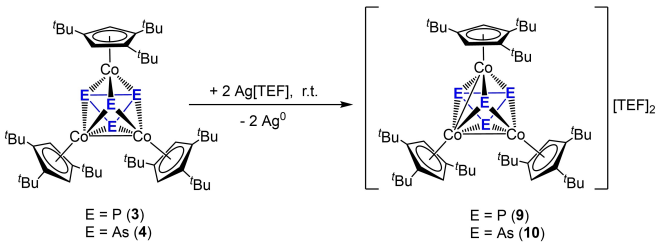

Scheme 4. Synthesis of the two-fold oxidized complexes **9** and **10**.

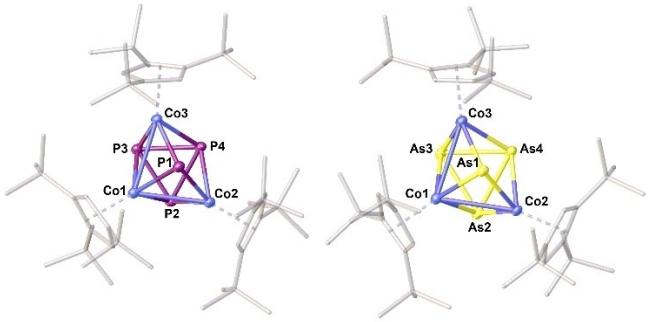

Figure 6. Molecular structures of the dications in **9** (left) and **10** (right) in the solid state. ADPs (anisotropic displacement parameters) are drawn at the 50 % probability level. Hydrogen atoms, anions and solvent molecules are omitted for clarity.

Complexes **9** and **10** possess each 60 VE, which matches the magic numbers for extraordinary stable complexes.

Crystals suitable for single crystal X-ray structure analysis are obtained from concentrated solutions in *ortho*-difluorobenzene layered with *n*-hexane at −30 °C after a few days. The molecular structures in the solid state are depicted in Figure 6.

The structures of **9** and **10** in the solid state reveal further changes in the transition metal cluster geometry upon oxidation. The trend observed for **8** is also valid for compounds **9** and **10**. In comparison to the monocations in **7** and **8**, the Co1–Co2 distance increases slightly (by 0.0674(8) Å (**9**) and 0.0271(8) Å (**10**), while the Co1–Co3 distance is significantly shortened (by 0.7278(9) Å (**9**) and 0.9399(7) Å (**10**)). Thus, the Co1–Co2 and Co1–Co3 distances in **9** and **10** are almost identical. In both dications, two strong metal-metal interactions are present as indicated by WBIs of 0.22 and 0.24 (**9**), 0.21 and 0.24 (**10**) and by the HOMO orbitals located mainly between Co1/Co2 and Co2/Co3 (cf. frontier orbitals in Figure S46 and S47). The E1 atom is shifted further into the direction of E4, while a stronger interaction between P1–P4 (2.5621(5) Å, WBI of 0.55) and As1–As4 (2.7612(7) Å, WBI of 0.55) is present. Both the distances P1–P4 and As1–As4 are now in the range of elongated single bonds,[12] but slightly longer than literature-known widened single bonds as in [(nacnacCu)$_2$(μ,η^2:η^2-E$_4$)] (P–P 2.4122(8)–2.4285(8), As–As 2.6562(4)–2.6617(4) Å).[14] The bond lengths within the E$_3$ units are similar to those in the monocations of **7** and **8**. Compound **9** and **10** are both diamagnetic. In the ^{1}H NMR spectra of **9** and **10**, all three singlets at δ = 5.41, 1.47 and 1.38 ppm (**9**) and δ = 5.07, 1.45 and 1.43 ppm (**10**) with an integral ratio of 6 : 54 : 27 are observed to be corresponding to three equivalent Cp‴ ligands in solution. In the ^{31}P{^{1}H} NMR spectrum of **9**, two broad singlets with an integral ratio of 1 : 3 at δ = 1104.3 and 489.7 ppm are detected.

Conclusions

In summary, we showed that the cluster complexes [(Cp‴Co)$_3$(μ_3,η^2:η^2:η^2-E$_3$)(μ_3-E)] (E = P (**3**), As (**4**)) can be synthesized via electrophilic quenching of **1** and **2** with [{Cp‴Co(μ-Cl)}$_2$]. The obtained novel homotrimetallic Co cluster complexes **3** and **4** show a distinct redox chemistry. One reduction and two oxidations were chemically realized for both compounds leading to salts containing the monoanions [K(L)(sol)$_n$][(Cp‴Co)$_3$(μ_3,η^2:η^2:η^2-E$_3$)(μ_3-E)] (E = P, L = 18cr6, sol = dme, n = 2 (**5**), E = As, L = 2,2,2-crypt, n = 0 (**6**)), monocations [(Cp‴Co)$_3$(μ_3,η^2:η^2:η^2-E$_3$)(μ_3-E)][FAl] (E = P (**7**), As (**8**)) and dications [(Cp‴Co)$_3$(μ_3,η^2:η^2:η^2-E$_3$)(μ_3-E)][TEF]$_2$ (E = P (**9**), As (**10**)). Upon reduction, the initial Co1–Co2 bond in **3** and **4** is cleaved by addition of electrons (**5**, **6**). In contrast, the removal of electrons in the first oxidation leads to only subtle changes in the geometry of the Co$_3$E$_4$ core for **7**, while the Co3 fragment is shifted strongly into the direction of the Co1 atom for **8**. In the second oxidation step, the withdrawal of an electron enforces the formation of one new Co–Co bond between Co1 and Co3 in the clusters **9** and **10**, respectively. However, both oxidation steps have no influence on the Co1-Co2 bond as opposed to

the reduction. As none of the explored redox processes lead to a fragmentation of the Co_3E_4 core of the clusters, compound **3** and **4** can be considered as electron reservoirs over four stages, where a range between 60 to 63 VE is covered.

Supporting Information Summary

The authors have cited additional references within the Supporting Information.[15] The supporting information includes details of the syntheses, spectroscopic and crystallographic characterizations of the products as well as details of the computations. Deposition Number(s) 2403273 (for **3**), 2403274 (for **4**), 2403275 (for **5**), 2403276 (for **6**), 2403277 (for **7**), 2403278 (for **8**), 2403279 (for **9**), 2403280 (for **10**) contain(s) the supplementary crystallographic data for this paper. These data are provided free of charge by the joint Cambridge Crystallographic Data Centre and Fachinformationszentrum Karlsruhe Access Structures service.

Acknowledgements

This work was supported by the Deutsche Forschungsgemeinschaft (DFG) within the projects Sche 384/36–2. C.R. is grateful to the Studienstiftung des Deutschen Volkes for a PhD fellowship. Benjamin Falge, Felix Riedlberger and Martin Weber are acknowledged for performing the cyclovoltammetry measurements. Open Access funding enabled and organized by Projekt DEAL.

Conflict of Interests

The authors declare no conflict of interest.

Data Availability Statement

The data that support the findings of this study are available in the supplementary material of this article.

Keywords: Arsenic · Cluster · Cobalt · Phosphorus · Redox chemistry

[1] a) P. Buchwalter, J. Rosé, P. Braunstein, *Chem. Rev.* **2015**, *115*, 28; b) A. W. Cook, Z. R. Jones, G. Wu, S. L. Scott, T. W. Hayton, *J. Am. Chem. Soc.* **2018**, *140*, 394; c) C. Iacobucci, S. Reale, J.-F. Gal, F. de Angelis, *Angew. Chem. Int. Ed.* **2015**, *54*, 3065; d) L. Jin, D. S. Weinberger, M. Melaimi, C. E. Moore, A. L. Rheingold, G. Bertrand, *Angew. Chem. Int. Ed.* **2014**, *53*, 9059; e) A. Makarem, R. Berg, F. Rominger, B. F. Straub, *Angew. Chem. Int. Ed.* **2015**, *54*, 7431; f) N. P. Mankad, *Chem. Comm.* **2018**, *54*, 1291; g) J. Oliver-Meseguer, J. R. Cabrero-Antonino, I. Domínguez, A. Leyva-Pérez, A. Corma, *Science* **2012**, *338*, 1452; h) J.-H. Jia, Q.-M. Wang, *J. Am. Chem. Soc.* **2009**, *131*, 16634; i) T. Murahashi, K. Shirato, A. Fukushima, K. Takase, T. Suenobu, S. Fukuzumi, S. Ogoshi, H. Kurosawa, *Nat. Chem.* **2012**, *4*, 52; j) M. Teramoto, K. Iwata, H. Yamaura, K. Kurashima, K. Miyazawa, Y. Kurashige, K. Yamamoto, T. Murahashi, *J. Am. Chem. Soc.* **2018**, *140*, 12682.
[2] J. Tang, L. Zhao, *Chem. Comm.* **2020**, *56*, 1915.
[3] a) O. J. Scherer, K. Pfeiffer, G. Heckmann, G. Wolmershäuser, *J. Organomet. Chem.* **1992**, *425*, 141; b) O. J. Scherer, G. Berg, G. Wolmershäuser, *Chem. Ber.* **1996**, *129*, 53.
[4] O. J. Scherer, S. Weigel, G. Wolmershäuser, *Chem. Eur. J.* **1998**, *4*, 1910.
[5] a) R. Ahlrichs, D. Fenske, K. Fromm, H. Krautscheid, U. Krautscheid, O. Treutler, *Chem. Eur. J.* **1996**, *2*, 238; b) C. von Hänisch, D. Fenske, F. Weigend, R. Ahlrichs, *Chem. Eur. J.* **1997**, *3*, 1494.
[6] C. Riesinger, L. Dütsch, M. Scheer, *Z. Anorg. Allg. Chem.* **2022**, *648*, e202200102.
[7] a) F. Dielmann, M. Sierka, A. V. Virovets, M. Scheer, *Angew. Chem. Int. Ed.* **2010**, *49*, 6860; b) F. Dielmann, A. Timoshkin, M. Piesch, G. Balázs, M. Scheer, *Angew. Chem. Int. Ed.* **2017**, *56*, 1671; c) C. Graßl, M. Bodensteiner, M. Zabel, M. Scheer, *Chem. Sci.* **2015**, *6*, 1379.
[8] M. Piesch, F. Dielmann, S. Reichl, M. Scheer, *Chem. Eur. J.* **2020**, *26*, 1518.
[9] S. B. Dinauer, R. Szlosek, M. Piesch, G. Balázs, S. Reichl, L. Prock, C. Riesinger, M. D. Walter, M. Scheer, *Dalton Trans.* **2024**, *53*, 10201.
[10] M. Piesch, C. Graßl, M. Scheer, *Angew. Chem. Int. Ed.* **2020**, *59*, 7154.
[11] a) D. M. P. Mingos, *Acc. Chem. Res.* **1984**, *17*, 311; b) K. Wade, *J. Chem. Soc. D.* **1971**, 792; c) K. Wade, *Advances in Inorganic Chemistry and Radiochemistry* (Hrsg.: H. J. Emeléus, A. G. Sharpe), Academic Press, **1976**, *18*, 1–66.
[12] P. Pyykkö, M. Atsumi, *Chem. Eur. J.* **2009**, *15*, 186.
[13] O. J. Scherer, K. Pfeiffer, G. Wolmershäuser, *Chem. Ber.* **1992**, *125*, 2367.
[14] F. Spitzer, M. Sierka, M. Latronico, P. Mastrorilli, A. V. Virovets, M. Scheer, *Angew. Chem. Int. Ed.* **2015**, *54*, 4392.
[15] a) Zhurko G. A., *Chemcraft - graphical software for visualization of quantum chemistry computations*; b) *Agilent, CrysAlisPro Software System Version 1.171.38.43, Agilent Technologies Ltd., Yarnton, Oxfordshire, England **2014***; c) D. Andrae, U. Häußermann, M. Dolg, H. Stoll, H. Preuß, *Theoret. Chim. Acta* **1990**, *77*, 123; d) F. Baumann, E. Dormann, Y. Ehleiter, W. Kaim, J. Kärcher, M. Kelemen, R. Krammer, D. Saurenz, D. Stalke, C. Wachter, et al., *J. Organomet. Chem.* **1999**, *587*, 267; e) A. D. Becke, *Phys. Rev. A* **1988**, *38*, 3098; f) O. V. Dolomanov, L. J. Bourhis, R. J. Gildea, J. A. K. Howard, H. Puschmann, *J. Appl. Cryst.* **2009**, *42*, 339; g) E. D. Glendening, C. R. Landis, F. Weinhold, *J. Comput. Chem.* **2013**, *34*, 1429; h) T. Köchner, N. Trapp, T. A. Engesser, A. J. Lehner, C. Röhr, S. Riedel, C. Knapp, H. Scherer, I. Krossing, *Angew. Chem. Int. Ed.* **2011**, *50*, 11253; i) I. Krossing, *Chem. Eur. J.* **2001**, *7*, 490. j) J.-M. Lalancette, G. Rollin, P. Dumas, *Can. J. Chem.* **1972**, *50*, 3058; k) Gaussian 06, M. J. Frisch, G. W. Trucks, H. B. Schlegel, G. E. Scuseria, M. A. Robb, J. R. Cheeseman, G. Scalmani, V. Barone, B. Mennucci, G. A. Petersson, H. Nakatsuji, M. Caricato, X. Li, H. P. Hratchian, A. F. Izmaylov, J. Bloino, G. Zheng, J. L. Sonnenberg, M. Hada, M. Ehara, K. Toyota, R. Fukuda, J. Hasegawa, M. Ishida, T. Nakajima, Y. Honda, O. Kitao, H. Nakai, T. Vreven, J. A. Montgomery, Jr., J. E. Peralta, F. Ogliaro, M. Bearpark, J. J. Heyd, E. Brothers, K. N. Kudin, V. N. Staroverov, T. Keith, R. Kobayashi, J. Normand, K. Raghavachari, A. Rendell, J. C. Burant, S. S. Iyengar, J. Tomasi, M. Cossi, N. Rega, J. M. Millam, M. Klene, J. E. Knox, J. B. Cross, V. Bakken, C. Adamo, J. Jaramillo, R. Gomperts, R. E. Stratmann, O. Yazyev, A. J. Austin, R. Cammi, C. Pomelli, J. W. Ochterski, R. L. Martin, K. Morokuma, V. G. Zakrzewski, G. A. Voth, P. Salvador, J. J. Dannenberg, S. Dapprich, A. D. Daniels, O. Farkas, J. B. Foresman, J. V. Ortiz, J. Cioslowski, and D. J. Fox, Gaussian, Inc., Wallingford CT, **2013**; l) J. P. Perdew, *Phys. Rev. B* **1986**, *33*, 8822; m) G. Scalmani, M. J. Frisch, *J. Chem. Phys.* **2010**, *132*, 114110; n) J. J. Schneider, D. Wolf, C. Janiak, O. Heinemann, J. Rust, C. Krüger, *Chem. Eur. J.* **1998**, *4*, 1982; o) G. M. Sheldrick, *Acta Crystallogr. Sect. A* **2008**, *64*, 112; p) G. M. Sheldrick, *Acta Crystallogr. Sect. A* **2015**, *71*, 3; q) G. M. Sheldrick, *Acta Crystallogr. Sect. C* **2015**, *71*, 3; r) S. Stoll, A. Schweiger, *J. Magn. Res.* **2006**, *178*, 42; s) J. Tomasi, B. Mennucci, R. Cammi, *Chem. Rev.* **2005**, *105*, 2999; t) F. Weigend, R. Ahlrichs, *Phys. Chem. Chem. Phys.* **2005**, *7*, 3297.

Manuscript received: November 26, 2024
Accepted manuscript online: January 8, 2025
Version of record online: ■■, ■■

RESEARCH ARTICLE

A straightforward synthesis of homotrimetallic Co polypnictogen cage complexes of the type $[(Cp'''Co)_3(\mu_3,\eta^2{:}\eta^2{:}\eta^2\text{-}E_3)(\mu_3\text{-}E)]$ (E = P (**3**), As (**4**)) is presented. These clusters were elucidated in terms of their redox chemistry by cyclic voltammetry. Stepwise reduction and oxidation over four stages give access to the corresponding salts containing monoanions, monocations and dications, which were comprehensively characterized in solution and in the solid state, respectively.

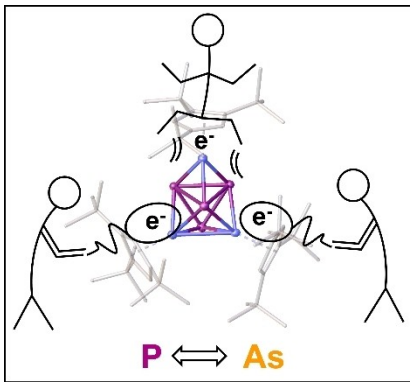

*M. Piesch, S. B. Dinauer, C. Riesinger, G. Balázs, M. Scheer**